Proceedings of the 2007 IEEE/RSJ International
Conference on Intelligent Robots and Systems
San Diego, CA, USA, Oct 29 - Nov 2, 2007

A Dynamic Single Actuator Vertical Climbing Robot

Amir Degani, Amir Shapiro, Howie Choset and Matthew T. Mason

Abstract— **A climbing robot mechanism is introduced, which uses dynamic movements to climb between two parallel vertical walls. This robot relies on its own internal dynamic motions to gain height, unlike previous mechanisms which are quasi-static. One benefit of dynamics is that it allows climbing with only a single actuated degree of freedom. We show with analysis, simulations and experiments that this dynamic robot is capable of climbing vertically between parallel walls. We introduce simplifications that enable us to obtain closed form approximations of the robot motion. Furthermore, this provides us with some design considerations and insights into the mechanism's ability to climb.**

I. INTRODUCTION

In recent years, several minimalist approaches to locomotion have been proposed. Some examples are hopping robots [1], [2] and passive dynamic walkers [3] designed with minimal number of active and passive joints. Reducing the number of actuators can simplify design, minimize weight and size of the mechanism, and reduce costs and risk of failure. Despite these advantages, few minimal mechanisms have been implemented for climbing robots. We propose a dynamic climbing mechanism which interacts with the environment (by shape and friction) to propel itself upwards against gravity using only one actuator with a simple open-loop control input. We focus on a two parallel wall environment which is similar to a channel or a crack in a wall (Fig. 1).

Using dynamic motions has two advantages in climbing. The first advantage is the ability to overcome obstacles which are impossible to pass in a quasi-static motion. One example is a human climber that cannot reach its next foothold. Leaping further using dynamic movements can help overcome this constraint. The second advantage of dynamic motions is in minimizing the number of actuators in a mechanism. We take advantage of this quality and use dynamic motions and implement a minimalist climbing mechanism. This mechanism consists of only two links. In order to climb it swings one of the links, which gives the whole system enough inertia change to climb upwards. The purpose of our analysis is to inspire future design of dynamic climbing mechanisms rather than as a purely applicable mechanism.

This work is sponsored in part by the Defense Advanced Research Projects Agency. This work does not necessarily reflect the position or the policy of the Government. No official endorsement should be inferred. This paper has a supplementary video of climbing simulation and experiments.

A. Degani, H. Choset and M.T. Mason are with the Robotics Institute, Carnegie Mellon University, Pittsburgh, PA 15213, USA <adegani,choset,matt.mason>@cs.cmu.edu

A. Shapiro is with the Department of Mechanical Engineering, Ben-Gurion University, Israel ashapiro@bgu.ac.il

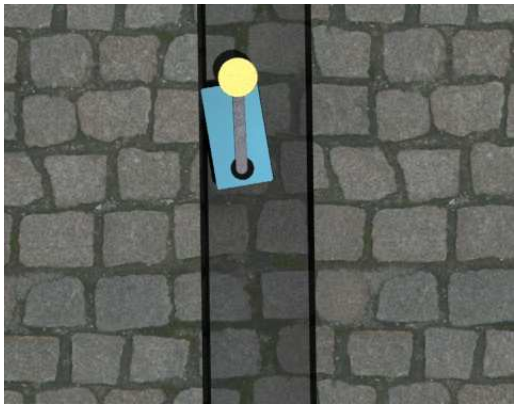

Fig. 1. Rendering of the robot dynamically climbing in a brick wall.

II. RELATED WORK

A. Climbing Robots

We review previous climbing robots in four groups according to the method they use to attach themselves to the environment: adhesive, spines, brute force fixture and "grasping". The adhesive group comprises of robots that use special mechanism such as electromagnetic fixtures on ferrous surfaces [4], suction [5], or other types of adhesives [6]. The spine group comprises of robots that use spines, and sometimes, micro-spines to attach themselves to surfaces [7]–[9]. The brute force fixtures include robots that use a special mechanism to grasp onto an engineered structure, such as a truss or pipe [10]. The last group of mechanisms, including our robot, uses its own kinematic and sometimes dynamic state to "grasp" itself into the environment. A typical example is a snake robot wedging itself inside a crack [11], or a multiple limb robot which uses frictional footholds to locomote [12], [13].

B. Dynamic Systems

Very few climbing systems have made use of dynamic motions. One recent example is [14], in which the authors designed and built a bio-inspired, two degree of freedom (DoF) vertical "running" robot assisted by springs. In manipulation and locomotion, however, dynamical systems are more often being used. In manipulation, Mason and Lynch [15] designed and controlled a minimalist single DoF mechanism to manipulate objects. In locomotion, Berkemeier and Fearing [2] and others introduced the Acrobot, based on Fredkin's hinge robot, which is a serial two-link robot, where the single actuated DoF is the second joint. The authors were able to control this mechanism and to make it hop and slide.

The mechanism we introduce in this paper is similar to the Acrobot in its simplicity, but also uses the constraints of the two parallel walls to propel itself vertically with a simple open-loop control.

III. ROBOT MODEL AND MODELING ASSUMPTIONS

In simulations and experiments this system exhibits stable periodic climbing motions. The goal of our analysis is to produce a model which exhibits behavior similar to that of the experiments and simulations. We intend to use this model to explore variant designs which can optimize the climbing characteristics of this mechanism with respect to the environment. The proposed mechanism is planar and consists of two links; the first is the main body which contacts the walls and the second is a pendulum which is connected to the main body through an actuated revolute joint (Fig. 2).

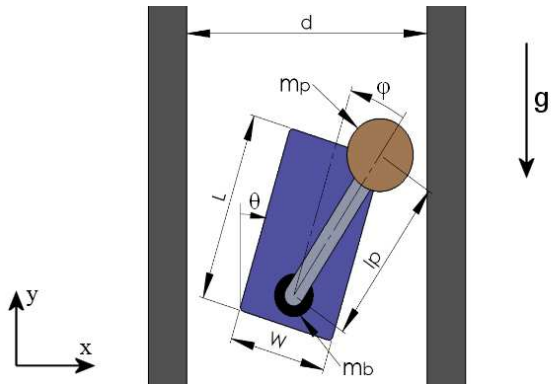

Fig. 2. Model of Robot.

Fig. 3 presents a dynamic simulation of two versions of the mechanism: both with the same size of the main body, but different pendulum length. The pendulum swings back and forth causing the main body to rotate. While doing so, the main body hits the walls and uses the dynamic movement of the pendulum to push itself upwards. When the pendulum is short as in Fig. 3a the climbing behaves in "purely dynamic" fashion, where the robot contacts the wall only with the two top corners of the main body. When the pendulum is longer (Fig. 3b) the robot's main body rotates after contact with the wall, and exhibits a "two point" contact phase. The focus of this paper will be on the former, simpler and more interesting "purely dynamic" movement. However, a similar analysis can be done on the other type of motion.

A few assumptions and design considerations will be made throughout the analysis of this mechanism based on the hypotheses described below. These enable us to obtain some closed form approximations of the mechanism's motion, and insights into the mechanism's design and ability to climb. First, the main body is comprised of a massless block (with width W and length L) and a point mass motor (m_b) at the hinge (we ignore reflected inertia and gear reduction). A pendulum, comprising a massless rod with a point mass (m_p) connected to it, is attached to the motor. The length of

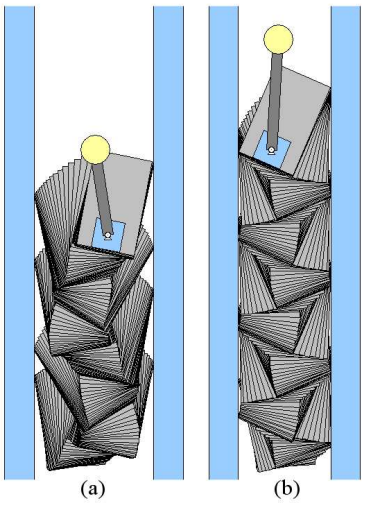

Fig. 3. Two typical motions of the dynamic climbing robot (the main body is traced over time) (a) Purely dynamic (single support) and (b) Double support.

the pendulum (l_p) is designed such that the pendulum mass will pass near the contact corners of the main body. θ is the angle of the main body relative to the vertical axis, and ϕ is the angle of the pendulum relative to the body (Fig. 2). The pendulum's trajectory is $\phi(t) = A\sin(\omega t)$, where A and ω are the pendulum's amplitude and angular frequency, respectively. We allow the pendulum mass to travel beyond the walls (technically, the pendulum can be out of the plane of the main body and the walls). The friction between the main body and the walls is very high, hence no slippage occurs.

IV. ANALYSIS

The dynamic equations of the mechanism can be described as:

$$M(q)\ddot{q} + N(q,\dot{q}) = \begin{bmatrix} 0 \\ 0 \\ 0 \\ \tau \end{bmatrix} - J^T(q)F_{ext}, \qquad (1)$$

where $q = (x, y, \theta, \phi) \in \mathbb{R}^2 \times \mathbb{S}^1 \times \mathbb{S}^1$ denote the generalized coordinates, $M(q) \in \mathbb{R}^{4\times4}$ is the symmetric inertia matrix, $N(q,\dot{q}) \in \mathbb{R}^4$ is the gravity effect, Coriolis and centrifugal forces, τ is the applied torque between the two links and F_{ext} is the contact force with the wall. Let $J(q) = \frac{\partial P(q)}{\partial q} \in \mathbb{R}^{2\times4}$ be the Jacobian matrix, where $P(q) = [P_x \quad P_y]^T$ is the point of contact with the walls. In the contactless case $F_{ext} = 0$.

To analyze the behavior of this robot in "purely dynamic" mode we will split the motion into three phases: impact, stance and flight phase (see Fig. 4). By using the final state of one phase as the initial values of the next phase we can analyze and simulate the climbing motion.

A. Impact Phase

A few model assumptions can be made to analyze the impact phase (as was done in [2], [19]). The impact model is

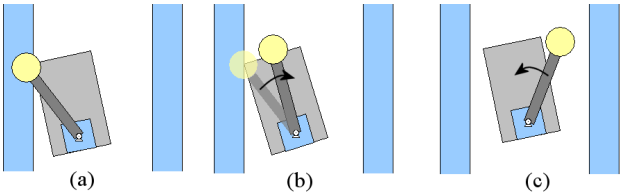

Fig. 4. Three phases: (a) impact (b) stance (c) flight.

assumed to be instantaneous and inelastic, where no slipping or rebound occurs during the impact. The external forces during the impact can be represented by impulses, which may result in an instantaneous change in the velocities but not in the configuration. In reality, actuators cannot generate impulsive torques and therefore can be ignored during the instantaneous time of impact. However, in our analysis we assume a known trajectory ($\phi(t) = A\sin(\omega t)$), therefore, we cannot neglect impulsive torques from the motors. Simulations and experiments in Section V support these hypotheses and assumptions.

The equations of impact can now be derived from (1) by integrating over the instantaneous time of impact, resulting in the simplified form

$$M(q)\Delta\dot{q} = [0 \quad 0 \quad 0 \quad I_\tau]^T - J^T(q)I_{Fext}, \qquad (2)$$

where I_{Fext} are the impulsive forces, I_τ is the impulsive torque, and $\Delta\dot{q}$ is the change of velocities over the time of impact. From (2), the velocity change during impact ($\Delta\dot{q}$) can be extracted by knowing I_τ and I_{Fext}.

Since finding I_τ and I_{Fext} is not trivial, we further simplify the analysis of this phase. As can be seen in the simulations and experiments section, in the case of our mechanism, the velocities after impact (including the angular velocities) almost completely vanish. This special occurrence is due to the body being hit inelastically in the center of percussion [17] and is not the general case of inelastic collision. When the impulsive force inelastically hits upon the center of percussion, rotations and translations of the body will completely stop. Therefore, in order to constrain the impact point to be on the center of percussion, a relationship between the geometry of the mechanism (l_p, L, W, A) and the mass distribution (m_b, m_p) can be found. Observing that the instantaneous center of rotation during the flight phase (prior to impact) is close to the bottom corner closest to the wall helps to evaluate the center of percussion.

B. Stance Phase

The stance phase is the segment where the main body is in contact with the wall, while the pendulum is swinging. One way to model this phase is by using the Lagrange multiplier method [18]. This method expresses the two contact forces (normal force F_x and tangential force F_y) as two variables as in (1). In order to solve for the four configuration space variables and these two contact forces, two new constraints are imposed. These constraints come from the assumption that no sliding occurs and therefore no work is done by the contact constraint forces, i.e.

$$J(q)\dot{q} = 0. \qquad (3)$$

Numerically solving this set of six differential equations will allow us to locate the configuration where the normal contact force (F_x) changes sign. This configuration is the change from stance to flight phase, and therefore the final state of the stance phase will be the initial state of the flight phase.

In order to find the state space of the system when transitioning to the flight phase we reduce the complexity of the six differential equations by using two observations. First, the main body hardly moves during stance phase. This is mainly due to the fact that we designed the mass of the pendulum to pass near the contact point (Fig. 4b) and that θ and ϕ during stance phase are small. This is similar to a two link serial manipulator with two identical links and two point masses at the end of each link. Solving the linearized system around $\theta = 0$ and $\phi = 0$ will result in negligible angle change of the first link. Because the velocity of the main body is negligible, the velocity of the center of mass (CoM) of the system depends only on the movement of the pendulum.

The second observation relates to the transition between the stance and the flight phases (as shown in Fig. 4b). Because the main body is nearly still during the stance phase and the pendulum's trajectory is a sine function, the transition point between these two phases occurs when $\phi = 0$. This is the configuration where the pendulum changes acceleration sign. From these two observations we can assume that the velocity of the CoM of the system just before transitioning to flight phase is $v_{CoM} = \frac{m_p v_p}{m_p + m_b}$ (where v_p is the pendulum's velocity). This velocity will be used as the initial velocity of the flight phase.

We next find the equation of the velocity of the mechanism transitioning between phases. Because the trajectory of the pendulum is $\phi(t) = A\sin(\omega t)$, the angular velocity is $\dot{\phi}(t) = A\omega\cos(\omega t)$, the velocity of the pendulum mass is $\dot{\phi} \times r_{p/H}$ (where $r_{p/H}$ is the vector from the hinge to the pendulum mass). Therefore $v_p = A\omega\cos(wt)\hat{k}\times(l_p\sin(\theta)\hat{i} + l_p\cos(\theta)\hat{j})$, where l_p is the length of the pendulum. By noticing that for the first half of the pendulum's cycle ($0 < t < \frac{\pi}{w}$) the main body will be hitting the left wall and for the second half of the cycle ($\frac{\pi}{w} < t < \frac{2\pi}{w}$) the main body will be hitting the right wall, we arrive at the equation that represents the velocity of the pendulum mass, and hence the velocity of the CoM of the whole system:

$$\begin{bmatrix} v_{xCoM} \\ v_{yCoM} \end{bmatrix} = \begin{bmatrix} -(\frac{m_p}{m_b+m_p})Al_p\omega\cos(\pi k)\cos(\theta_{\text{trans}}) \\ (\frac{m_p}{m_b+m_p})Al_p\omega\cos(\pi k)\sin(\theta_{\text{trans}}) \end{bmatrix}, \qquad (4)$$

where θ_{trans} is the angle of the main body in the transition between stance phase and flight phase from the left wall ($k = 1$), or from the right wall ($k = 2$).

C. Flight Phase

We now know the initial velocities of the CoM in flight phase and can turn to analyzing the motion of the mechanism

while "leaping" between the two walls. By considering the CoM of the system as the origin of the inertial frame during the flight phase, this phase can be decoupled into a simple projectile (parabolic) motion of the CoM and an internal shape change of the mechanism. Given the initial velocities of the CoM (obtained in (4)) the trajectory of the CoM will draw a parabola in each "leap" between the two walls:

$$x_{CoM} = x_{0CoM} + v_{xCoM}t \tag{5}$$

$$y_{CoM} = y_{0CoM} + v_{yCoM}t - \frac{1}{2}gt^2, \tag{6}$$

where x_{0CoM} and y_{0CoM} are the initial locations of the CoM.

In order to know when the main body will hit the opposite wall, we need to identify the relationship between the orientations of the two links (θ and ϕ). Given that in free flight the angular momentum is conserved, we can derive the relationship [2], [20]:

$$K_1(\phi)\dot{\theta} + K_2(\phi)\dot{\phi} = H, \tag{7}$$

where H is the angular momentum, and K_1 and K_2 are functions of ϕ. When the robot is released for the first time from rest in flight phase, angular momentum (H) is zero. For this special case there is a closed form solution to (7) (we refer the reader to the appendix of [20] for a solution to this case). In all other occurrences of the flight phase, the angular momentum is not zero because the main body is motionless at liftoff while the pendulum is moving. In this general case ($H \neq 0$) (7) is a nonholonomic constraint. Thus, this equation cannot be integrated to the form of $f(q) = 0$. However, because we know that the explicit trajectory of the pendulum is $\phi(t) = A\sin(\omega t)$, (7) becomes integrable and hence $\theta(t)$ can be computed.

The observed motion of the mechanism in steady state is symmetric relative to the walls, and the transition angle (θ_{trans}) will be constant for all stance phases. Therefore, the approximate horizontal distance of the CoM from the wall during transition is $r_{CoMx/wall} \simeq \frac{W}{2\cos(\theta_{\text{trans}})}$. This approximation is accurate when the pendulum mass is larger than the motor mass and when θ_{trans} is small. We can now calculate the trajectory of the mechanism in flight phase. By substituting $|v_x|$ from (4) and the horizontal distance that the CoM can pass between the walls into (5), we arrive at the equation that provides the time (T) it takes for the CoM to reach the opposite wall.

$$T = \left(\frac{d - \frac{W}{2\cos(\theta_{\text{trans}})}}{(\frac{m_p}{m_b+m_p})Al_p\omega\cos(\theta_{\text{trans}})} \right), \tag{8}$$

where d is the distance between the two walls and W is the width of the main body. The nominator $d - \frac{W}{2\cos(\theta_{\text{trans}})}$ is approximately the horizontal distance that the CoM can pass between the walls. Inserting (8) and $|v_y|$ from (4) into (6) gives the equation for the incremental "leap" in the y direction between the two walls:

$$\Delta y = \tan(\theta_{\text{trans}}) \left(d - \frac{W}{2\cos(\theta_{\text{trans}})} \right) - \frac{1}{2}gT^2. \tag{9}$$

It is difficult to precisely calculate θ_{trans}. One approach, which we do not implement here, is to find this angle by analyzing the converging limit cycle and interpreting this angle from it.

By assuming that the body rotates approximately around the bottom corner of the main body (closer to the wall), and that the hinge joint will be roughly at half the distance between the two walls because the mechanism motion is symmetric relative to the walls, we can arrive at an equation which allows us to approximate θ_{trans}. To do so, we approximate that the hinge is located at the bottom edge of the main body.

$$L\sin(\theta_{\text{trans}}) + \frac{W}{2}\cos(\theta_{\text{trans}}) = \frac{d}{2}, \tag{10}$$

where L is the length of the mechanism. Solving for θ_{trans} will give the approximate angle at which the robot hits the walls. The simulations and experiments provide support that this assumption is realistic and that this approximation is reasonable.

V. SIMULATIONS AND EXPERIMENTS

A. Simulations

In order to verify our analysis, and our assumptions, we have simulated the climber using the Working Model 2D dynamic simulator (Design Simulation Technologies, Inc). These simulations use the Kutta-Merson numerical integration method with variable integration step size to simulate the motion. We will present a few representative results of the simulations with a typical robot with these parameters: $W = 0.04\,\text{m}$, $L = 0.065\,\text{m}$, $l_p = 0.0585\,\text{m}$, $m_b = 0.1\,\text{kg}$, $m_p = 0.2\,\text{kg}$, $A = 0.5\,\text{rad}$, $\omega = 70\,\text{rad/sec}$, $d = 0.08\,\text{m}$, $g = 9.807\,\text{m/sec}^2$.

Fig. 5 depicts a phase plot of one full cycle of the mechanism's motion. Fig. 5a is the phase plot of the main body, and Fig. 5b is the phase plot of the pendulum. Distance between two tick marks represents 10 msec.

A closeup of the main body's phase plot depicting the three phases is shown in Fig. 6. Supporting our previous assumptions, it can be seen that during the impact phase the angular velocities almost vanish instantaneously and during the stance phase there is barely any movement of the main body. The flight phase depicts a "leap" to the opposite wall. As can be seen, the landing angle on one wall is identical to the angle on the other (with opposite signs).

A comparison of the CoM's trajectory during one "leap" taken from the Working Model 2D simulation to the "leap" from (4), (5), (6), (8) is shown in Fig. 7. In order to verify the incremental vertical "leap" (9), we insert into it the parameters of the robot resulting in $\Delta y = 0.01\,\text{m}$, which is close to the simulation results ($\Delta y = 0.012\,\text{m}$). Note that $\theta_{\text{trans}} = 0.33\,\text{rad}$ was calculated using (10).

B. Experiments

We built a prototype of the dynamic climbing mechanism, as shown in Fig. 8. The main body is built out of very low mass balsa wood. A Hitec HSR-5995TG high torque motor is connected to the wood and drives the pendulum.

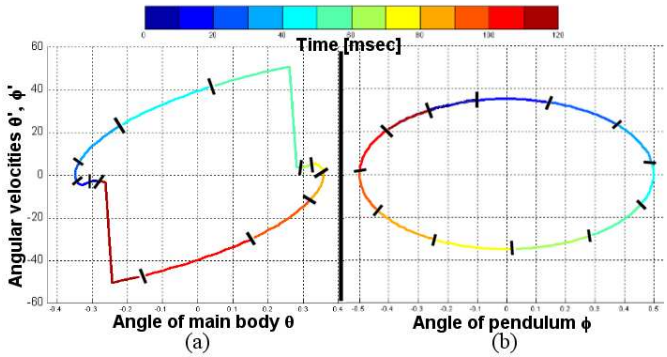

Fig. 5. Phase plots of (a) main body, (b) pendulum.

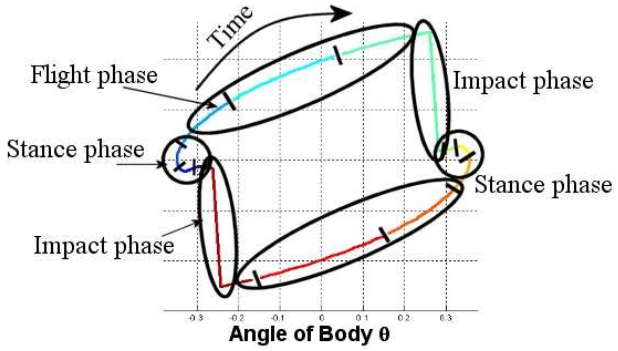

Fig. 6. Phase plot closeup of the main body in simulation (the three phases are marked).

A large variable mass is connected to the pendulum. In order to decrease the out-of-plane motions during impact, the mass of the pendulum is designed to be as close as possible to the impact plane. In order to control the amount of gravitational acceleration, we placed the mechanism on an inclined frictionless air-table. The air-table also helps keep the mechanism planar. To increase the contact surface area of the main body with the air-table, we attached a 15 cm plastic disc to the main body.

The purely dynamic motion was tested successfully on a relatively low inclined air-table (0.1 rad and 0.6 rad).

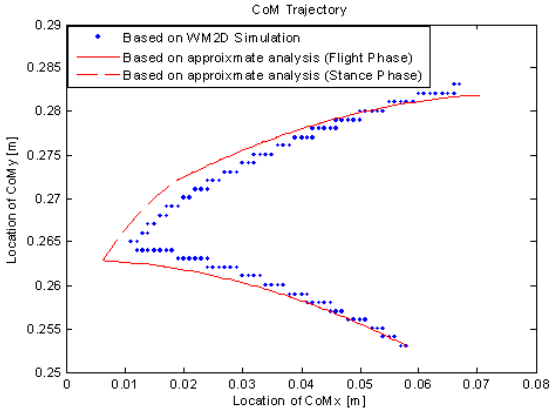

Fig. 7. Trajectory of the CoM during two leaps.

These lower gravitational fields helped lower motor speeds. Fig. 9 shows a few frames of the experiment held on a 0.1 rad incline with these parameters: $W = 0.03\,\text{m}$, $L = 0.065\,\text{m}$, $l_p = 0.12\,\text{m}$, $m_b = 0.07\,\text{kg}$, $m_p = 0.1\,\text{kg}$, $A = 0.3\,\text{rad}$, $\omega = 25\,\text{rad/sec}$, $g = 9.807\,\text{m/sec}^2$, $d = 0.06\,\text{m}$. Perturbations of the mechanism stabilized in less than two cycles.

In this experiment the mechanism progressed approximately 0.005 m per leap. For comparison, we inserted the parameters of the experiments into (9) and approximated the leap in the vertical direction to be 0.007 m. Considering that friction and other disturbances were not taken into account these are very satisfying results.

After completing the initial experiment we conducted a successful experiment with a high incline ($\approx 80°$). This was done with the two phase motion because this type of motion requires slower motor speed. Fig. 8 shows a snapshot of the climber in the experimental setup. It was important to keep the incline angle less than $90°$ in order to ensure contact with the frictionless air-table, and to avoid out-of-plane motions and contact of the plastic disc with the walls.

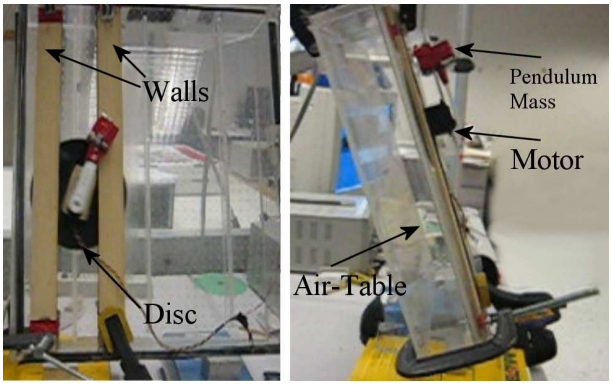

Fig. 8. Experimental setup: The air-table is on an $80°$ incline.

VI. FUTURE WORK AND CONCLUSION

We have introduced a new dynamic mechanism that uses a single DoF to climb between two vertical walls. Some assumptions were used in order to simplify the equations of motion and hence make them tractable. A few of these assumptions, such as allowing the pendulum to cross over the walls, can be avoided by decreasing the amplitude and increasing the angular frequency. This was not implemented due to the limitations of our current motors.

Through a detailed analysis we have identified a few design and motor parameters, together with environment parameters, which determine the incremental vertical leap. Experiments and simulations have verified the analysis and showed that this mechanism is able to climb in a dynamic fashion with a single actuated DoF.

In future work we intend to improve the design to eliminate the use of the air-table. In order to do so, we must overcome the challenge of keeping the robot planar. One possible solution would be to place the climber inside a tube which is axisymmetric, therefore small rotations around the

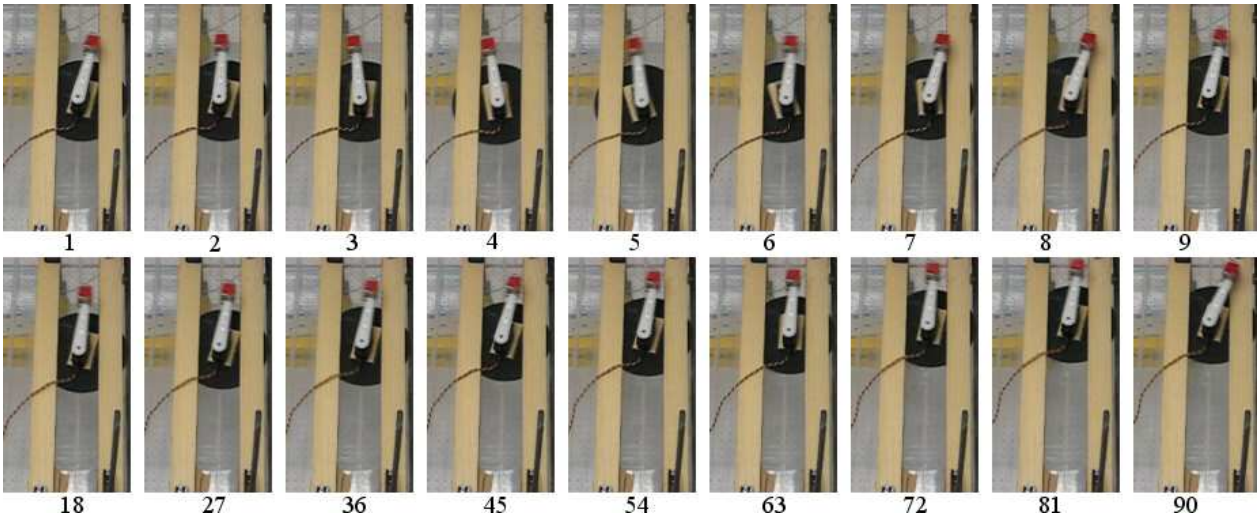

Fig. 9. Frames from experiment: 0.1 rad, $m_b = 70$ gr, $m_p = 100$ gr, ≈30 frames per second. The first row depicts one full cycle of the mechanism's climbing motion, while the second row depicts the configuration of the mechanism at the end of nine consecutive cycles.

main axis will not change the contact of the robot with the environment. Another future direction might be to change the way the mechanism impacts the walls. A more elastic impact can improve power efficiency and can be analyzed with a compliance contact model. Furthermore, although the assumption we made of a stable mechanism was verified in simulations and experiments, a proof of stability criteria of the mechanism is warranted.

Lastly, in this paper we assumed an open-loop input which enabled the robot to climb between two parallel walls. We intend to extend this work by implementing a control law which will enable the mechanism to plan and execute its own motion in a non-uniform environment, e.g. pegs in random locations or piecewise linear walls.

Climbing has many facets, such as mechanism design, gait control, motion planning and dynamic motions. We believe that dynamic climbing can be very advantageous, for example by minimizing the number of actuators and overcoming obstacles. To the best of our knowledge, this mechanism is the first climbing mechanism to use a single actuator to climb dynamically.

REFERENCES

[1] M.H. Raibert, *Legged Robots That Balance*, The MIT Press, Cambridge, MA; 1986.

[2] M.D. Berkemeier and R.S. Fearing, Sliding and Hopping Gaits for the Underactuated Acrobot, *IEEE Transactions on Robotics and Automation.*, vol. 14, 1998, pp 629-634.

[3] T. McGeer, Passive Dynamic Walking, *The International Journal of Robotics Research*, vol. 9, no. 2, 1990, pp 62-82.

[4] L. Guo, K. Rogers and R. Kirkham, "A Climbing Robot with Continuous Motion", *Proceedings of the IEEE International Conference on Robotics and Automation, (ICRA '94)*, San Diega, CA, 1994, pp. 2495-2500.

[5] S. Hirose and K. Kawabe, "Ceiling Walk of Quadruped Wall Climbing Robot NINJA-II", *Proceedings of the 1st International Conference on Climbing and Walking Robots, (CLAWAR '98)*. Brussels, Belguim, 1998, pp. 143-147.

[6] K.A. Daltorio, A.D. Horchler, S. Gorb, R.E. Ritzmann and R.D. Quinn, "A Small Wall-Walking Robot with Compliant, Adhesive Feet", *Intelligent Robots and Systems (IROS 2005), IEEE/RSJ International Conference on*, Edmonton, Canada, 2005, pp. 152-159.

[7] S. Kim, A.T. Asbeck, M.R. Cutkosky and W.R. Provancher, "SpinybotII: Climbing Hard Walls With Compliant Microspines", *Proceedings of the 12th International Conference on Advanced Robotics, (ICAR '05)*. Seattle, WA, 2005, pp. 601-606.

[8] K. Autumn, et al., "Robotics in Scansorial Environments", *Proceedings of SPIE Vol. 5804 Unmanned Ground Vehicle Technology VII.*, 2005, pp. 291-302.

[9] G. La Spina, C. Stefanini, A. Menciassi, P. Dario, Novel Technological Process for Fabricating Micro Tips for Biomimetic Adhesion, *Journal of Micromechanics and Microengineering*, vol. 15, 2005, pp 1576-1587.

[10] M. Abderrahim, C. Balaguer, A. Gimenez, J.M. Pastor and V.M. Padron, "ROMA: A Climbing Robot for Inspection Operations", *Proceedings of the IEEE International Conference on Robotics and Automation, (ICRA '99)*, Detroit, MI, 1999, pp. 2303-2308.

[11] A. Greenfield, A.A. Rizzi, H. Choset, "Dynamic Ambiguities in Frictional Rigid-body Systems with Application to Climbing via Bracing", *Proceedings of the IEEE International Conference on Robotics and Automation, (ICRA '05)*, Barcelona, Spain, 2005, pp. 1947- 1952.

[12] T. Bretl, Motion Planning of Multi-Limbed Robots Subject to Equilibrium Constraints: The Free-Climbing Robot Problem, *International Journal of Robotics Research*, vol. 25, No. 4, 2006, pp 317-342.

[13] A. Shapiro, E. Rimon, S. Shoval, PCG: A Foothold Selection Algorithm for Spider Robot Locomotion in 2D Tunnels, *International Journal of Robotics Research*, vol. 24, No. 10, 2005, pp. 823-844.

[14] J.E. Clark, D.I. Goldman, T.S Chen, R.J. Full, and D. Koditschek, "Toward a Dynamic Vertical Climbing Robot", *Proceedings of the 9th International Conference on Climbing and Walking Robots, (CLAWAR '06)*, Brussels, Belgium, 2006.

[15] M.T. Mason and K.M. Lynch, "Dynamic Manipulation", *Intelligent Robots and Systems, (IROS '93). IEEE/RSJ International Conference on*, Yokohama, Japan, 1993, pp. 152-159.

[16] R. Balasubramanian, A.A. Rizzi, M.T. Mason, "Legless Locomotion: Models and Experimental Demonstration", *Proceedings of the IEEE International Conference on Robotics and Automation, (ICRA '04)*, New Orleans, LA, 2004, pp. 1803- 1808.

[17] R.L. Norton, *A Design of Machinery: An Introduction to the Synthesis and Analysis of Mechanisms and Machines*, McGraw-Hill, New York, NY; 2004.

[18] R.M. Murray, Z. Li and S. Sastry, *A Mathematical Introduction to Robotic Manipulation*, CRC Press, Boca Raton, FL; 1994.

[19] I.D. Walker, "The Use of Kinematic Redundancy in Reducing Impact and Contact Effects in Manipulation", *Proceedings of the IEEE International Conference on Robotics and Automation, (ICRA '90).* Cincinnati, OH, 1990, pp. 434-439 .

[20] C. Frohlich, Do Springboard Divers Violate Angular Momentum Conservation?, *American Journal of Physics*, vol. 47, No. 7, 1979, pp. 583-592.